Highly selective phenol production from benzene on a platinum-loaded tungsten oxide photocatalyst with water and molecular oxygen: selective oxidation of water by holes for generating hydroxyl radical as the predominant source of the hydroxyl group

AUTHOR(S):

Tomita, Osamu; Ohtani, Bunsho; Abe, Ryu

CITATION:

Tomita, Osamu ...[et al]. Highly selective phenol production from benzene on a platinum-loaded tungsten oxide photocatalyst with water and molecular oxygen: selective oxidation of water by holes for generating hydroxyl radical as the predominant source of the hydroxyl group. Catalysis Science & Technology 2014, 4(11): 3850-3860

ISSUE DATE:

2014-05-02

URL:

http://hdl.handle.net/2433/198293

Journal Name
Dynamic Article Link

Cite this: DOI: 10.1039/c0xx00000x

www.rsc.org/xxxxxx

ARTICLE TYPE

Highly selective phenol production from benzene on platinum-loaded tungsten oxide photocatalyst with water and molecular oxygen: Selective oxidation of water by holes for generating hydroxyl radical as predominant source of hydroxyl group

Osamu Tomita,[a,b] Bunsho Ohtani[b] and Ryu Abe*[a,c]

Received (in XXX, XXX) Xth XXXXXXXXX 20XX, Accepted Xth XXXXXXXXX 20XX
DOI: 10.1039/b000000x

Particles of tungsten oxide loaded with nanoparticulate platinum (Pt/WO_3) photocatalytically produced phenol from benzene with high selectivity (e.g., 74% at 69% of benzene conversion) in water containing molecular O_2; the selectivity for phenol were much higher than those on conventional titanium oxide (TiO_2) photocatalysts (both the unmodified and Pt-loaded) that generated CO_2 as a main product. Results confirmed that photoexcited electrons in the Pt/WO_3 photocatalysts mainly generated H_2O_2 from molecular O_2 through a two-electron reduction; the H_2O_2 generated did not significantly contribute to the undesirable peroxidation of phenol produced. In contrast, the oxygen radical species, such as $\bullet O_2^-$ or $\bullet HO_2$, generated on TiO_2 photocatalysts partially contributed to the successive oxidation of phenol and other intermediates to reduce the selectivity toward phenol. More importantly, the reactions using ^{18}O-labeled O_2 and H_2O clearly revealed that the holes generated on Pt/WO_3 react primarily with H_2O molecules, even in the presence of benzene in aqueous solution, selectively generating •OH radicals that subsequently react with benzene to produce phenol. In contrast, a portion of holes generated on TiO_2 photocatalysts reacts directly with benzene molecules, which are adsorbed on the surface of TiO_2 by strong interaction with surface hydroxyl groups. This direct oxidation of substances by holes undoubtedly enhanced non-selective oxidation, consequently lowing selectivity for phenol by TiO_2. The two unique features of Pt/WO_3, the absence of reactive oxygen radical species from O_2 and the ability to selectively oxidize water to form •OH, are the most likely reasons for the highly selective phenol production.

1. Introduction

Chemical syntheses using semiconductor photocatalysts can be environmentally benign processes that possess great potential for reducing energy consumption in industrial production of useful chemicals by using light energy.[1-3] The high reduction and oxidation potentials of photoexcited electrons and holes, respectively, generated on semiconductor particles such as TiO_2 can promote various chemical reactions, even endothermic reactions. Another advantage of photocatalytic organic syntheses is the availability of molecular oxygen (O_2) or water (H_2O) as abundant and harmless reductants or oxidants, instead of conventional, expensive reductants and oxidants that generally generate non-recyclable wastes requiring separation from the products. Molecular O_2 is an efficient electron acceptor (*i.e.*, oxidant) for the photoexcited electron generated on TiO_2 photocatalysts, where the holes generated can directly oxidize the organic substances adsorbed, and can indirectly oxidize through formation of •OH radicals from H_2O molecules adsorbed on the surface; the •OH radicals generated subsequently oxidize the organic substances to produce desired products.[2, 4-11] However, TiO_2 photocatalysts generally exhibit high activity for non-selective and complete oxidation of organic compounds in the presence of ambient O_2, yielding CO_2 and highly oxidized products.[2, 12-18] This property is very useful for mineralization of toxic organic compounds, but is detrimental to the development of highly selective organic synthetic systems. Only a limited number of highly selective organic synthesis using conventional TiO_2 photocatalysts in the presence of molecular O_2 has been reported.[19, 20] The low selectivity for the desired products is due to the competitive nature of successive oxidations of products, as well as the raw materials and intermediates through undesirable pathways.[21, 22] Some oxygen radical species, such as $\bullet O_2^-$ or $\bullet HO_2$ generated from O_2 molecules *via* reaction with photoexcited electrons, are thought to contribute to the oxidation of organic substances to some extent.[23-30] Some research groups have reported highly selective organic synthesis using TiO_2-related photocatalysts in the absence of molecular O_2.[31-34] For example, Shiraishi *et al.* demonstrated highly selective synthesis of benzimidazoles from *ortho*-phenylenediamine and ethanol using Pt-loaded TiO_2 photocatalyst (Pt/TiO_2) under UV light irradiation.[31] Yoshida *et al.* reported direct hydroxylation of benzene to phenols using Pt/TiO_2 suspended in water containing a high concentration of substances such as benzene (*e.g.*, 1:1 v/v),

in which selectivity for hydroxylation of benzenes was greatly improved because the reaction was conducted in the absence of molecular O_2.[32] In these reactions on Pt/TiO_2 photocatalysts, protons (H^+) were used as an electron acceptor instead of molecular O_2, accompanied by production of H_2 on Pt cocatalysts. Although these reports might indicate the potential of highly selective organic synthesis through the use of photocatalysts, reaction efficiencies generally decreased significantly due to the reduced ability of H^+ as an electron acceptor compared to O_2. Furthermore, the potential of H^+ reduction requires a highly negative conduction band minimum (CBM) of the semiconductor, and therefore limits the applicable semiconductor materials to TiO_2. The use of TiO_2 photocatalysts is limited in practical applications by their wide bandgaps (*ca*. 3.2 eV for anatase, *ca*. 3.0 eV for rutile) that require UV light irradiation for excitation. The energy efficiencies in artificial UV light sources, such as high-pressure Hg lamps or UV-LEDs, are low and insufficient for achieving cost-effective chemical synthesis using TiO_2 photocatalysts. Thus, using visible light is desired for the lower cost provided by efficient visible light sources such as blue-LEDs as well as for the possibility of using natural sunlight.

Previous studies have demonstrated that particles of tungsten oxide (WO_3) loaded with nanoparticulate platinum (Pt) exhibit photocatalytic activity sufficient for oxidation of various organic compounds under visible light; the activity was similar to that of TiO_2 under UV light.[35] Although WO_3 generally has been regarded as a photocatalyst inactive for oxidation of organic compounds with molecular O_2 due to insufficient CBM for reduction of O_2, the loading of nanoparticulate Pt cocatalyst significantly increases the probability of multi-electron reduction of O_2 by photoexcited electrons, enhancing the oxidation of organic substances by the holes remaining in the valence band. The photoexcited electrons in Pt-loaded WO_3 (Pt/WO_3) were suggested to produce mainly H_2O_2 *via* two-electron reduction. These findings led to the application of the Pt/WO_3 photocatalyst to organic synthesis reactions because it is activated under visible light but does not generate oxygen radicals such as $\bullet O_2^-$ or $\bullet HO_2$, which may enhance the peroxidation of products. The direct hydroxylation of benzene to phenol was selected as the target reaction because it is one of the most challenging chemical reactions. The present industrial synthesis of phenol, the major source of phenol resins, is based on the cumene method–a multi-step process that requires a large amount of energy. Therefore, direct, one-step synthesis of phenol from benzene is a desirable process and has been studied extensively. The Pt/WO_3 photocatalysts recently have been shown to possess activity for direct production of phenol from benzene using O_2 and water as reactants under UV or visible light.[36] Selectivity toward phenol on Pt/WO_3 photocatalysts was much greater than that on Pt/TiO_2 (or unmodified TiO_2) photocatalyst; however, reasons for the differences in reactivity and selectivity of the two photocatalysis systems are not known.

The present study examined the reaction mechanism of highly selective phenol production from benzene on Pt/WO_3 photocatalysts in detail compared to that on TiO_2 (including Pt-loaded TiO_2) to find the contributing factors. Results revealed that the holes generated in the WO_3 photocatalysts possess distinctly different reactivity from those in TiO_2 toward oxidation and hydroxylation of benzene, regardless of their similar oxidation potentials, enabling highly selective phenol production from benzene in water.

2. Experimental Section

2.1. Samples

Commercially available WO_3 powders, such as WO_3-K (triclinic and monoclinic, 4.8 $m^2\ g^{-1}$, Kojundo Chemical Laboratory), WO_3-Y (monoclinic, 2.2 $m^2\ g^{-1}$, Yamanaka Chemical Industries), and WO_3-S (monoclinic, 1.6 $m^2\ g^{-1}$, Soekawa Chemicals), were used. The fine particulate WO_3 sample, referred to as WO_3-K (triclinic, 10 $m^2\ g^{-1}$), was obtained by separation from large aggregates by mean of centrifugation of the purchased WO_3-K samples as previously reported.[35] The TiO_2 powders, such as TiO_2-P [anatase and rutile, P 25, 55 $m^2\ g^{-1}$, Degussa (Evonik)], TiO_2-A (anatase, 10 $m^2\ g^{-1}$, Merck), and TiO_2-R (rutile, 4.0 $m^2\ g^{-1}$, Aldrich), were used.

2.2. Platinum loading using the photodeposition method

Samples loaded with Pt nanoparticles were prepared as follows. The sample powder was stirred in an aqueous methanol solution (10 vol%) containing the required amount of H_2PtCl_6 as a Pt precursor. The WO_3 samples were irradiated with visible light; the TiO_2 samples were irradiated with UV and visible light. After washing several times with distilled water, the sample was dried in air at 353 K for 12 h. The diameters of Pt nanoparticles loaded were confirmed to be 3 ~ 10 nm as demonstrated in the previous study.[35]

2.3. Photocatalytic reaction

Photocatalytic reaction of benzene was conducted in a Pyrex reaction cell (15 mL) in an aerated aqueous benzene solution (water volume: 7.5 mL; initial benzene amount: 18.8 μmol) with continuous stirring at 279 K. The source for both the ultraviolet and visible light was a 300-W Xenon lamp so that results could be compared with those for TiO_2 photocatalysts ($300 < \lambda < 500$ nm). Sample aliquots were withdrawn from the reactor cell after each irradiation and filtered through a PVDF filter (Mini-Uni Prep™) to remove photocatalyst particles. Product analysis was performed using a high performance liquid chromatograph equipped with a C-18 column and photodiode-array detector (Shimadzu, SPD-M20A). Generation of carbon dioxide in the gas phase was analyzed using a gas chromatograph (Shimadzu, GC-14B) equipped with a flame-ionization detector.

The amount of H_2O_2 produced during photocatalytic oxidation of an organic substrate was analyzed by iodometry.[37] The photocatalyst (10 mg) suspended in 10 mL water was placed in a Pyrex test tube (30 mL) in the presence of ambient oxygen. The initial amount of acetic acid (as hole scavenger) was 300 μmol. After irradiation of the photocatalyst suspension, 2 mL of solution was removed with a syringe and the photocatalyst separated from the solution using a syringe PVDF filter (Millex®W). Then 1 mL of 100 mmol L^{-1} aq. potassium hydrogen phthalate ($C_8H_5KO_4$) and 1 mL of 400 mmol L^{-1} aq. potassium iodide (KI) were added. The H_2O_2 was allowed to react with I^- under acidic conditions ($H_2O_2 + 3I^- + 2H^+ \rightarrow I_3^- + 2H_2O$). The amount of H_2O_2 was determined by the maximum intensity of absorption attributed to I_3^- at approximately 350 nm, measured using a UV-Vis spectrophotometer (Shimadzu UV-1800).

For tracer studies, either $H_2{}^{18}O$ (98 atom%, Taiyo Nippon Sanso Corp.) or $^{18}O_2$ (98 atom%, Taiyo Nippon Sanso Corp.) gas was used as the oxygen isotope source. Then, 50 mg of photocatalyst suspended in 1 mL $H_2{}^{18}O$ (in air) or $H_2{}^{16}O$ (in $^{18}O_2$) was used. In the case of reactions in $H_2{}^{16}O$ solvent with $^{18}O_2$ gas, the solution was purged with Ar gas and subsequently with $^{18}O_2$ gas to make the partial pressure of O_2 in the reaction system similar to that in air; the amount of N_2 gas was under the detection limit in each reaction. The initial amount of benzene used to investigate the hydroxylation process of benzene to phenol was 500 μmol (500 mmol L^{-1}). After the photocatalyst suspended in solution had been irradiated, a portion (20 μL) was extracted by syringe, added to diethyl ether (300 μL) containing the internal standard, and shaken in a tube mixer. The amount of ^{18}O-labeled phenol was determined using GC-MS (Shimadzu, GCMS-2010/PARVUM2).

2.4. IR measurements

FT-IR spectra of the adsorbed benzene on each sample were recorded with a Fourier-transform infrared spectrometer (Jasco FT-4200). The sample pellet was introduced into an IR cell equipped with CaF_2 windows. Prior to the measurements, the sample was heated in vacuum. After cooling, benzene vapor was introduced into the cell and then evacuated in the gas phase. The spectra obtained after adsorption of benzene were subtracted from the corresponding spectra before adsorption.

3. Results and Discussion

3.1. Hydroxylation of benzene over various Pt/WO_3 and Pt/TiO_2 photocatalysts

Figure 1 shows the time course of photocatalytic hydroxylation and oxidation of benzene on Pt-loaded WO_3 and Pt-loaded TiO_2 samples in water (7.5 mL) containing saturated air and a small amount of benzene (*ca*. 18.8 μmol). Reactions were started with the benzene concentration (2.5 mmol L^{-1}) sufficiently lower than the maximum soluble value of benzene in water (22.3 mmol L^{-1}), in order to accurately quantify the reduced amount of benzene during each reaction.[38] Upon irradiation with UV and visible light, the amount of benzene decreased, while the rate and the order of reaction varied among the samples. Selectivity for each product was distinctly different for the Pt/WO_3 and Pt/TiO_2 systems.

Phenol and CO_2 were the predominant products in the Pt/WO_3 and Pt/TiO_2 systems, respectively. For Pt/WO_3-K (Fig. 1a), phenol was produced at an almost steady rate under irradiation along with small amounts of di-hydroxylated benzenes (not plotted) and CO_2.

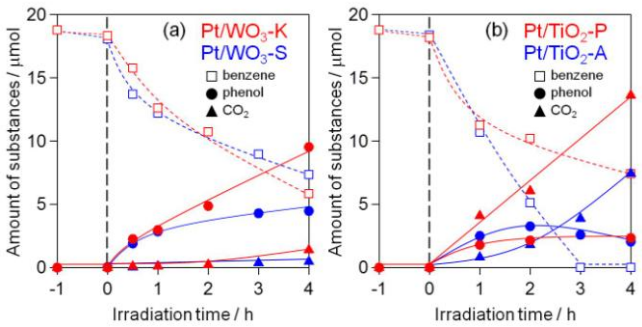

Figure 1. Time course of photocatalytic oxidation of benzene over (a) Pt/WO_3 and (b) Pt/TiO_2 photocatalysts in aerated aqueous solutions of benzene (18.8 μmol) under ultraviolet and visible light irradiation (300 < λ < 500 nm).

Table 1. Conversion and phenol selectivity for hydroxylation of benzene[a]

Entry	Photocatalyst	Conversion (%)[b] (Irradiation time / h)	Selectivity (%)[c] Phenol	Catechol	Resorcinol	Hydro quinone	Benzo quinone	Amount of CO_2 / μmol
1	Pt/WO_3-K	22.2 (1)	79.3	1.9	0	1.2	4.0	< 0.1
		68.9 (4)	73.7	2.3	0.7	0	8.8	1.4
2	Pt/WO_3-Y	40.6 (1)	58.8	1.2	0	1.3	1.1	<0.1
		63.6 (4)	57.1	1.4	0	2.2	0.5	0.4
3	Pt/WO_3-S	32.4 (1)	48.7	1.2	0	2.0	1.2	0.6
		59.2 (4)	41.7	1.2	0	2.1	0.0	1.1
4	WO_3-K	16.4 (4)	84.6	1.6	0	3.3	1.1	<0.1
5[d]	Pt/WO_3-K	26.6 (1)	83.8	1.4	0	1.2	2.8	< 0.1
		52.5 (4)	75.1	1.4	0	2.9	1.2	0.6
6	Pt/TiO_2-P	38.0 (1)	25.9	0	0	0.6	1.1	4.1
		59.1 (4)	21.8	0	< 0.1	0.8	0.1	13.6
7	Pt/TiO_2-A	43.0 (1)	31.0	2.8	0	1.9	0	0.8
		99.0 (4)	10.9	4.2	0.3	2.1	0	7.5
8	Pt/TiO_2-R	24.1 (1)	36.9	3.2	0	9.1	1.7	1.5
		76.8 (4)	11.9	2.6	0.1	5.9	1.7	3.7
9	TiO_2-P	51.6 (1)	22.7	0	0	1.4	0.2	4.7
		82.5 (4)	20.6	< 0.1	0	0.8	0.1	13.4
10	TiO_2-A	37.8 (1)	23.6	3.4	0	3.0	0	0.4
		84.5 (4)	14.5	5.7	0.1	2.8	0	4.9
11	TiO_2-R	34.1 (1)	24.8	1.6	0	11.5	0	1.8
		68.3 (4)	16.1	1.6	0	6.7	0	12.5

[a]Initial amount of benzene : 18.8 μmol, solvent : H_2O 7.5 mL, light source : 300 W Xe lamp, [b]Conversion : $(C_{benzene,0} - C_{benzene,t})/C_{benzene,0} \times 10^2$, [c]Selectivity : $C_{products,t}/(C_{benzene,0} - C_{benzene,t}) \times 10^2$, [d]Under visible light irradiation($400 < \lambda < 500$ nm) .

Table 1 summarizes the selectivity for each product, calculated on the basis of the decrease in benzene. Because selectivity for CO_2 is difficult to determine due to uncertainty in the stoichiometry between the decrease in benzene and generation of CO_2, the amount of CO_2 generated is listed in Table 1. Selectivity for phenol by the Pt/WO_3-K photocatalyst (entry 1) initially (1 h) was *ca*. 79%, with a benzene conversion of 22%, along with appreciable production of catechol (1.9%), hydroquinone (1.2%), and *p*-benzoquinone (4.0%). The generation of CO_2 was below the detection limit (< 0.1 μmol). Even with high benzene conversion (64%) after a long period of irradiation (4 h), selectivity for phenol was high (74%), while the amount of CO_2 became detectable (*ca*. 1.4 μmol). The Pt/WO_3-K photocatalyst had high selectivity for hydroxylated benzene or quinone throughout the reaction period (*ca*. 86.4% and 85.5% after 1 and 4 h of irradiation, respectively). The products without an aromatic ring were not quantified because quantification by HPLC was difficult, even with a photodiode array detector. Therefore, the unidentified fraction (*ca*. 14%) reflected the cleaved intermediates, including oxidized CO_2. Other Pt/WO_3 samples also generated phenol as the main product with relatively high selectivity and a negligibly small amount of CO_2 (Figs. 1a and S1a, and Table 1) in the initial period (1 h), while the Pt/WO_3-S sample showed significantly lower selectivity (*ca*. 42%) after 4-h irradiation. These findings strongly suggest that the rate of successive oxidation of phenol on Pt/WO_3 photocatalysts, specifically on Pt/WO_3-K sample, is lower than that of hydroxylation of benzene, affording high selectivity for phenol.

In contrast, CO_2 was predominantly generated on Pt/TiO_2-P (Fig. 1b) at a steady rate during the initial period along with an appreciable amount of phenol. The amount of phenol nearly reached saturation after 1 h of photo-irradiation, indicating

successive oxidation of the phenol once produced to give cleaved intermediates and CO_2. The production of CO_2 during the initial period strongly suggests a direct oxidation pathway of benzene without the formation of any hydroxylated intermediates such as phenol. Selectivity for phenol was quite low (26%) on Pt/TiO_2-P, even at short irradiation times (1 h) with relatively low conversion of benzene (Table 1, entry 6). The use of other Pt/TiO_2 samples also resulted in predominant production of CO_2, along with much lower selectivity for phenol (Figs. 1b and S1, Table 1) than that of Pt/WO_3. However, the time courses for CO_2 and phenol production were different from that using Pt/TiO_2-P. For example, use of Pt/TiO_2-A (Fig. 1b) generated predominantly phenol during the initial period, followed by generation of CO_2 along with a gradual decrease in phenol amount, indicating successive oxidation of the phenol produced. Similar reactivity was observed for the Pt/TiO_2-R sample with the pure rutile phase (Fig. S1). Selectivity for phenol on these Pt/TiO_2 photocatalysts (Table 1, entries 6-8) was much lower than that on Pt/WO_3 photocatalysts. Note that the Pt/WO_3-K and the Pt/TiO_2-A samples, which have similar surface areas (*ca*. 10 m^2 g^{-1}), possessed different reactivities. Thus, the factor dominating reactivity is related to the difference in the composition (WO_3 or TiO_2), not on the surface area.

These results indicate that the rates of successive oxidation of phenol on Pt/WO_3 photocatalysts are much lower than those on Pt/TiO_2 photocatalysts, enabling Pt/WO_3 to produce phenol with high selectivity. Another advantage of the Pt/WO_3 photocatalysts is the ability to use it with visible light irradiation. As shown in Table 1, visible light irradiation (λ > 400 nm) afforded better phenol selectivity (entry 5) than did full arc irradiation (entry 1) on Pt/WO_3-K photocatalyst, with a comparable reaction rate. For Pt/TiO_2-P with mixed anatase and rutile phase, an appreciable decrease in benzene amount was observed (Fig. S2) certainly due to reaction on the rutile phase that can absorb light up to *ca*. 410 nm, while the rate was much lower than that under UV light irradiation (Fig. 1). As expected based on the photoabsorption properties of TiO_2 anatase, visible light irradiation of Pt/TiO_2-A did not yield any appreciable products (Fig. S2).

3.2. Influence of oxygen-reduced species on phenol selectivity by Pt/WO_3 and Pt/TiO_2 photocatalysts

The Pt/WO_3 photocatalysts exhibited significantly greater selectivity for phenol production than did the Pt/TiO_2 system, which showed high activity for oxidative degradation of benzene and other intermediates including phenols. A possible reason for the difference in reactivity between the two systems could be a difference in level of participation of the O_2 reduced species (H_2O_2, $\bullet O_2^-$, or $\bullet HO_2$), generated during the reductive process by photoexcited electrons, in the oxidation of benzene or intermediates. The conduction band minimum (CBM) of WO_3 semiconductor (*ca*. +0.5V *vs*. SHE) was much lower than the potentials of O_2 reduction *via* the one-electron process [$O_2 + e^- \rightarrow \bullet O_2^-$, $E^0(O_2/\bullet O_2^-) = -0.28$ V; or $O_2 + H^+ + e^- \rightarrow \bullet HO_2$, $E^0(O_2/\bullet HO_2) = -0.05$ V vs. SHE], resulting in rapid recombination between photoexcited electrons and holes in WO_3 photocatalysts even in the presence of a sufficient amount of O_2. Unmodified WO_3 samples indeed exhibited a low rate of benzene oxidation and hydroxylation, but the selectivity toward phenol was adequate (Table 1, entry 4). However, loading of highly dispersed Pt nanoparticles on WO_3 was shown to significantly enhance the rate of oxidative decomposition of aliphatic compounds, such as acetaldehyde, under visible light. This enhancement is due to promotion of multi-electron reduction of O_2 [$O_2 + 2e^- + 2H^+ \rightarrow H_2O_2$, $E^0(O_2/H_2O_2) = +0.68$ V; or $O_2 + 4e^- + 4H^+ \rightarrow 2H_2O$, $E^0(O_2/H_2O) = +1.23$ V vs. SHE] on Pt cocatalysts; these reactions are able to proceed thermodynamically, even through the photoexcited electrons generated in the conduction band of WO_3. The small amount of Pt loading (0.1 wt.%) also was effective for enhancing the rate of hydroxylation and oxidation of benzene on Pt/WO_3-K photocatalysts, strongly suggesting the occurrence of multi-electron reduction of O_2 on Pt cocatalyst in the present system. As shown in Fig. S3, the optimum amount of Pt loading for phenol production was *ca*. 0.1 wt.%; greater amounts resulted in lower selectivity for phenol and increased generation of CO_2, while the reaction rate was increased.

In contrast, TiO_2 semiconductors possess much more negative CBM (anatase: ca. –0.2 V, rutile: ca. +0.05 V vs. SHE) than that of WO_3. These values, especially that of anatase, are considered sufficient for progress of O_2 reduction *via* a single-electron process by assuming a shift in the CBM potentials of TiO_2 under near neutral pH conditions.[39] Most TiO_2 photocatalysts, especially those with anatase, exhibit sufficiently high activity for oxidative degradation of various organic compounds even without a cocatalyst such as Pt. In the present system, unmodified TiO_2-P photocatalyst exhibited greater conversion of benzene than that loaded with 0.1 wt.% of Pt (see Table 1 and Fig. S3), implying that most of the photoexcited electrons were consumed on the TiO_2 surface, even with Pt loading, *via* single-electron processes producing radical species of O_2 (*e.g.*, $\bullet O_2^-$ or $\bullet HO_2$). As shown in Fig. S3, selectivity for phenol on TiO_2 photocatalysts was minimally affected by Pt loading amount, while the conversion of benzene on Pt/TiO_2-A increased significantly with Pt loading amount. Thus, an amount of 0.1 wt.% Pt loading in the TiO_2 system was a reasonable value for comparison with the Pt/WO_3 system.

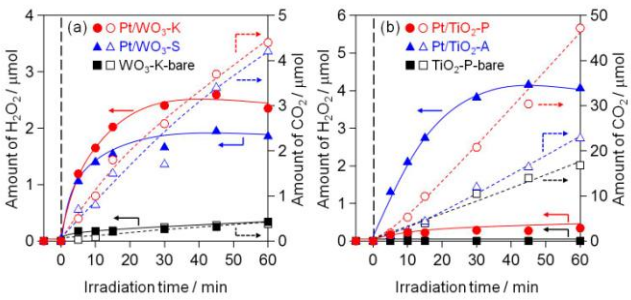

Figure 2. Time course curves of H_2O_2 and CO_2 generation over (a) WO_3 and (b) TiO_2 photocatalysts suspended in AcOH solution under ultraviolet and visible light irradiation (300 < λ < 500 nm).

Products generated from molecular O_2 during the reduction on WO_3 and TiO_2 were evaluated using the photocatalytic oxidation of acetic acid in aqueous solution containing O_2. Figure 2 shows time courses for H_2O_2 and CO_2 production over WO_3 and TiO_2 photocatalysts suspended in aqueous acetic acid (AcOH) under both ultraviolet and visible light irradiation (300 < λ < 500 nm).

(Time courses for other samples are shown in Fig. S4.) Under irradiation, both H_2O_2 and CO_2 were simultaneously generated on unmodified and Pt-loaded WO_3 samples, while the rates were much greater with the Pt-loaded samples. Saturation of H_2O_2 on Pt/WO_3 samples was undoubtedly due to the catalytic decomposition of H_2O_2 into H_2O and O_2 on Pt particles, with a possible contribution of photocatalysis by electrons or holes. Assuming that CO_2 generation occurred only by photogenerated holes ($CH_3COOH + 2H_2O + 8H^+ \rightarrow 2CO_2 + 8H^+$), combining this process with H_2O_2 generation ($O_2 + 2H^+ + 2e^- \rightarrow H_2O_2$) should result in generation of H_2O_2 and CO_2 with the ideal stoichiometric ratio of 2:1 ($CH_3COOH + 2H_2O + 4O_2 \rightarrow 4H_2O_2 + 2CO_2$). As summarized in Table 2, the ratio of amount of H_2O_2 generated to that of CO_2 was close to the stoichiometric value, both on unmodified and Pt-loaded WO_3-K samples (2.4 and 2.1), indicating that most of the photoexcited electrons on WO_3-K were consumed *via* the two-electron reduction of O_2, producing H_2O_2. Other Pt/WO_3 samples also showed appreciable generation of H_2O_2 with CO_2, while the rates of H_2O_2 production were lower than the stoichiometric value expected from the CO_2 generation. This deviation is likely due to the catalytic and/or photocatalytic decomposition of H_2O_2, and possibly the four-electron reduction of O_2 to H_2O on Pt cocatalyst.

Table 2. Initial production rate of H_2O_2 and CO_2 over WO_3 and TiO_2 photocatalysts suspended in aq. AcOH.[a]

Entry	Photocatalyst	Amount of H_2O_2 production / μmol	Amount of CO_2 production / μmol	Ratio of amount of H_2O_2 to CO_2
1	Pt/WO_3-K	1.2	0.5	2.4
2	Pt/WO_3-Y	1.1	0.7	1.4
3	Pt/WO_3-S	0.6	0.5	1.1
4	Pt/TiO_2-P	0.2	1.8	0.1
5	Pt/TiO_2-A	1.3	1.2	1.1
6[b]	Pt/TiO_2-R	0.9	1.0	0.9
7[b]	WO_3-K	0.2	0.1	2.1
8	TiO_2-P	0	1.2	0
9	TiO_2-A	0.2	0.7	0.3
10[b]	TiO_2-R	0.1	0.1	1.2

[a]Initial amount of AcOH : 300 μmol, amount of solvent (H_2O) : 10 mL light source : 300 W Xe lamp ($300 < \lambda < 500$ nm), calculated on the amount of products after 5 min, [b]Calculated on the amount of products after 10 min.

In contrast, the generation of H_2O_2 on TiO_2-P was negligibly low, independent of Pt loading, despite the high rates of CO_2 generation (Fig 2 and Table 2, entries 4, 8). These results indicate that photoexcited electrons on the TiO_2-P photocatalyst were consumed mainly *via* one-electron processes producing radical species ($\bullet O_2^-$ or $\bullet HO_2$), although four-electron reduction of O_2 to form H_2O on the Pt-loaded sample also was possible. On other TiO_2-A and TiO_2-R samples, H_2O_2 generation was appreciable, especially after Pt loading, indicating enhanced two-electron reduction of O_2 on Pt cocatalyst.

Comparison of the results shown in Tables 1 and 2 indicate a connection between selectivity for H_2O_2 generation from aq. AcOH and selectivity for phenol from benzene. The TiO_2 samples with low selectivity for H_2O_2 production (*e.g.*, unmodified TiO_2-P, Pt/TiO_2-P) that indicated high selectivity for oxygen radical species ($\bullet O_2^-$ or $\bullet HO_2$) tended to exhibit low selectivity for phenol production from benzene. However, samples with high selectivity for H_2O_2 generation (*e.g.*, Pt/TiO_2-A, Pt/TiO_2-R) exhibited appreciably higher selectivity for phenol. These findings suggest that the oxygen radical species ($\bullet O_2^-$ or $\bullet HO_2$) generated on TiO_2 samples contributed to oxidative decomposition of the substrates and consequently lowered selectivity for phenol. Although the contribution of these oxygen radical species toward oxidation of organic compounds is not well understood, the oxidative reactivity of radical species ($\bullet O_2^-$ or $\bullet HO_2$) should be greater than that of non-radical H_2O_2. Some studies have suggested that the $\bullet O_2^-$ species generated during photocatalysis on TiO_2 enhanced the cleavage of aromatic rings.[30] However, the generation of reactive oxygen radical species is suppressed on the Pt-WO_3 systems by the lower CBM, which forces reduction of O_2 molecules into H_2O_2 or H_2O *via* a multi-electron process.

These results have prompted the hypothesis that the high selectivity for phenol on Pt/WO_3 is due to the absence of reactive oxygen radical species ($\bullet O_2^-$ or $\bullet HO_2$), which enhances oxidative decomposition of the phenol or other intermediates produced. This hypothesis is supported by the results from photocatalytic oxidation and hydroxylation of benzene in the absence of molecular O_2, which are summarized in Table 3. For the Pt/WO_3 system, reactions were conducted in the presence of Ag^+ as an electron acceptor instead of O_2, because it possess an appropriate potential [+0.799 V vs. SHE] for efficient scavenging of photoexcited electrons generated in WO_3. Since the addition of $AgNO_3$ (18.8 μmol) makes the aqueous solution acidic (pH ～5), the influence of pH on phenol selectivity needs to be considered. Phenol selectivity of the Pt/WO_3-K samples was reduced by decreasing pH value (Fig. S5). Therefore, results for Pt/WO_3-K samples in the presence of O_2 (*i.e.*, in the absence of Ag^+) at different pH values are included in Table 3 for comparison.

Table 3. Hydroxylation of benzene over WO_3 photocatalysts in the absence of molecular O_2.[a]

Entry	Reaction conditions	Photocatalyst	Conversion (%) (Irradiation time / h)	Phenol selectivity (%)
Ref. 1	O_2, pH~6	Pt/WO_3-K	22.2 (1)	79.3
Ref. 2	O_2, pH~5	Pt/WO_3-K	18.9 (1)	55.4
1	Ag^+, Ar	Pt/WO_3-K	27.5 (1) 53.0 (3)	54.0 51.5
2	Ag^+, Ar	Pt/WO_3-Y	40.8 (1) 72.3 (3)	50.1 50.3
3	Ag^+, Ar	Pt/WO_3-S	46.9 (1) 71.1 (3)	48.2 51.5
4	H^+, Ar	Pt/TiO_2-P	13.3 (1) 33.8 (4)	60.8 34.0
5	H^+, Ar	Pt/TiO_2-A	10.8 (0.3) 27.4 (4)	51.9 26.1
6	H^+, Ar	Pt/TiO_2-R	11.6 (1) 25.8 (4)	41.8 27.2
7	Ag^+, Ar	TiO_2-P-bare	19.8 (0.5)	50.5

[a] Initial amount of benzene : 18.8 μmol, initial amount of Ag^+ ion : 18.8 μmol, amount of solvent (H_2O) : 7.5 mL, light source : 300 W Xe lamp ($300 < \lambda < 500$ nm)

Interestingly, selectivity for phenol by the Pt/WO_3 system was minimally affected by the presence of O_2; similar values for phenol selectivity were obtained with or without O_2, even at different reaction times (*i.e.*, at different levels of benzene conversion). These findings strongly suggest that the H_2O_2

generated by the Pt/WO_3 system *via* reduction of O_2 did not significantly contribute to the undesirable peroxidation of phenol. These results also imply that the existence of O_2 in the reaction media, whether it is reduced or not, has no impact on phenol selectivity. In contrast, the existence of O_2 significantly decreased selectivity of phenol by the Pt/TiO_2 system. For the Pt/TiO_2 system, reactions were initiated in deaerated water containing only benzene, without adding any electron acceptor, because the CBM of TiO_2, especially that of anatase, is sufficient for reduction of water (or H^+) to H_2 (generation of H_2 was confirmed for all the Pt/TiO_2 samples). As summarized in Table 3, selectivity toward phenol by the Pt/TiO_2 samples was improved significantly by conducting the reactions in the absence of O_2, while the conversions at same reaction time lower compared to those with O_2 (see Table 1) primarily due to the lower reaction rate of photoexcited electron with H^+ than that with O_2. For example, phenol selectivity on Pt/TiO_2-P was improved significantly from 26 to 61% during the initial period (Table 1, entry 6; Table 3, entry 4). Yoshida *et al.* also demonstrated improved phenol selectivity using Pt/TiO_2 photocatalyst in a deaerated solution of benzene and water (1:1 by vol.).[32] The same tendency was observed on unmodified TiO_2-P in the presence of an Ag^+ electron acceptor (Table 3, entry 7); selectivity for phenol was improved from *ca*. 23% (Table 1, entry 9) to 50% at 30 min of reaction by removing O_2 from solution. These findings strongly support the hypothesis that the oxygen radical species ($\bullet O_2^-$ or $\bullet HO_2$) generated on TiO_2 contributed to oxidative decomposition of the substrate including phenol, consequently lowering selectivity for phenol. However, selectivity for phenol in the Pt/TiO_2 system decreased significantly upon prolonged reaction time, even in the absence of O_2 (Table 3, entries 4-6), in contrast to results for the Pt/WO_3 system. These results suggest that factors other than the reactive oxygen radical species contribute to the difference in reactivity between Pt/WO_3 and Pt/TiO_2 (including unmodified TiO_2) for hydroxylation and oxidation of benzene. The most likely cause is the difference in reactivity of the holes generated in each photocatalyst system. To clarify the reasons for the reactivity differences, specifically the difference in selectivity of holes for phenol production on the WO_3 and TiO_2 systems, the reaction mechanism for each system was investigated in detail using ^{18}O-labeled O_2 and H_2O.

3.3. Determination of oxygen sources for phenol production from benzene on Pt/WO_3 and Pt/TiO_2 systems using ^{18}O-labeled O_2 and H_2O

In general, photocatalytic hydroxylation of benzene to phenols is considered to proceed through two different routes as illustrated in Schemes 1 and 2.[2, 40-44] The first route (Scheme 1) is initiated by photocatalytic generation of hydroxyl radicals (•OH) from H_2O molecules and/or surface hydroxyl groups of the semiconductor, which then react with benzene molecules to yield benzene radical species (Radical I). The benzene radical species then reacts with another •OH in solution or a hole on the semiconductor to produce a phenol. If phenol production proceeds through this route, the O atoms originally contained in the H_2O molecules of the solvent must be introduced into the phenol. The route shown in Scheme 2, which has been suggested recently by Matsumura *et al.*,[43] is initiated by direct oxidation of benzene molecules on the semiconductor surface with photo-generated holes, giving cationic radical species of benzene (Radical II). The cationic radical species then are attacked by O_2 or $\bullet O_2^-$ molecules to give peroxidized species. The peroxidized species then are transformed into phenol molecules accompanied by proton (H^+)-coupled reduction with photoexcited electrons (e^-), as shown in Scheme 2. In this case, the phenol molecules produced must contain O atoms originating from the molecular O_2 dissolved in the solution. To clarify the dominant route operating in phenol production on Pt/WO_3 and Pt/TiO_2 systems, reactions were conducted using a stable oxygen isotope (^{18}O-enriched water: $H_2{}^{18}O$, or $^{18}O_2$).

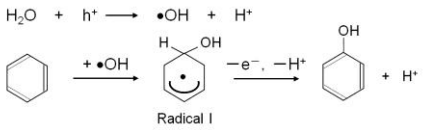

Scheme 1. Proposed reaction for phenol production over photocatalysts *via* hydroxyl radical.

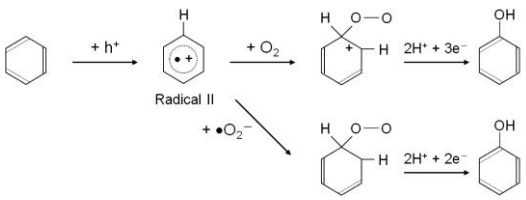

Scheme 2. Proposed reaction for phenol production over photocatalysts *via* oxygen molecule and oxygen radical.

Figures 3 and S7 show time courses for production of phenol from benzene by photocatalysis using four Pt/WO_3 and Pt/TiO_2 samples, conducted in ^{18}O-enriched water (1.0 mL, 98% $H_2{}^{18}O$) containing benzene and molecular O_2 ($^{16}O_2$). Total amount of phenol produced and percentage of phenol containing ^{18}O were plotted against irradiation time. A larger amount of benzene (500 μmol) was added to the water for these reactions compared to that for reactions shown in Fig. 1, to minimize successive peroxidation of phenol. Photoirradiation of Pt/WO_3-K produced phenol at a nearly steady rate; percentage of ^{18}O-labeled phenol was greater than 90% throughout the reaction, while the percentage decreased slightly from 95% (15 min) to 91% (8 h) during the reaction (Table 4, entry 1). The high percentage of ^{18}O-labeled phenol throughout the reaction indicated that phenol production on Pt/WO_3-K proceeded primarily *via* a reaction pathway involving hydroxyl radicals (•OH) from $H_2{}^{18}O$ molecules, which were the source of ^{18}O in the phenol produced (Scheme 1). The slight decrease in percentage of ^{18}O-labeled phenol during the reaction was probably due to the increased amount of $H_2{}^{16}O$ molecules, which were generated directly by four-electron reduction of $^{16}O_2$ or indirectly by catalytic decomposition of $H_2{}^{16}O_2$ on Pt; the $H_2{}^{16}O$ molecules produced subsequently were used as a source of O atoms for phenol through formation of •OH radicals. As shown in Fig. 4, reaction in unlabeled $H_2{}^{16}O$ solvent containing labeled $^{18}O_2$ molecules resulted in preferential production of unlabeled phenol molecules (*ca*. 95% at 15 min and 90% at 8 h). When the reaction was conducted in $H_2{}^{16}O$-$H_2{}^{18}O$ (1:1) containing unlabeled $^{16}O_2$, the percentage of ^{18}O-labeled phenol was slightly less than 50% throughout the reaction (Fig. S6; Table 4, entry 7).

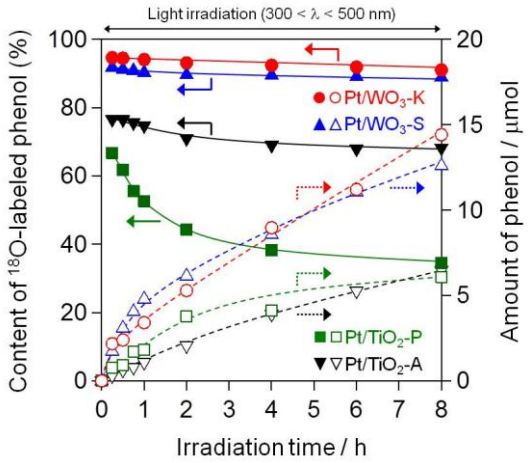

Figure 3. Time course of photocatalyzed production of phenol from benzene on Pt/WO_3 and Pt/TiO_2 samples. Reactions were conducted in ^{18}O-enriched water (98% $H_2{}^{18}O$) containing benzene and normal molecular $^{16}O_2$.

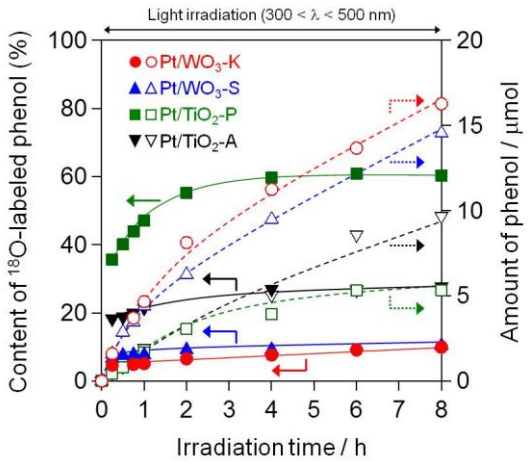

Figure 4. Time course of photocatalyzed production of phenol from benzene on Pt/WO_3 and Pt/TiO_2 samples. Reactions were conducted in normal water ($H_2{}^{16}O$) containing benzene and molecular $^{18}O_2$.

Table 4. Direct hydroxylation of benzene in $H_2{}^{18}O$ in the presence of $^{16}O_2$

Entry	Photocatalyst	Reaction Condition	Content of labeled phenol (%) (Amount of phenol produced / μmol)	
			15 min	8 h
1	Pt/WO_3-K	$^{16}O_2$, $H_2{}^{18}O$	94.7 (2.2)	91.1 (14.4)
2	Pt/WO_3-Y	$^{16}O_2$, $H_2{}^{18}O$	92.7 (1.0)	88.6 (11.9)
3	Pt/WO_3-S	$^{16}O_2$, $H_2{}^{18}O$	92.5 (1.7)	88.9 (12.6)
4	Pt/TiO_2-P	$^{16}O_2$, $H_2{}^{18}O$	66.8 (0.8)	34.5 (6.1)
5	Pt/TiO_2-A	$^{16}O_2$, $H_2{}^{18}O$	76.6 (0.3)	68.2 (6.5)
6	Pt/TiO_2-R	$^{16}O_2$, $H_2{}^{18}O$	74.5 (0.1)	47.3 (1.2)
7	Pt/WO_3-K	$^{16}O_2$, $H_2{}^{16}O$: $H_2{}^{18}O$ = 1 : 1	46.3 (1.2)	43.9 (14.9)
8	Pt/TiO_2-P	$^{16}O_2$, $H_2{}^{16}O$: $H_2{}^{18}O$ = 1 : 1	31.6 (0.4)	16.7 (5.9)
9	Pt/WO_3-K	$^{18}O_2$, $H_2{}^{16}O$	4.6 (1.6)	9.9 (16.3)
10	Pt/WO_3-Y	$^{18}O_2$, $H_2{}^{16}O$	6.9 (1.4)	8.6 (13.2)
11	Pt/WO_3-S	$^{18}O_2$, $H_2{}^{16}O$	6.7 (1.6)	10.4 (14.6)
12	Pt/TiO_2-P	$^{18}O_2$, $H_2{}^{16}O$	35.7 (0.4)	60.4 (5.3)
13	Pt/TiO_2-A	$^{18}O_2$, $H_2{}^{16}O$	18.2 (0.5)	27.7 (9.7)
14	Pt/TiO_2-R	$^{18}O_2$, $H_2{}^{16}O$	25.8 (0.1)	53.2 (1.5)

Initial concentration of benzene : 500 μmol, amount of solvent : 1.0 mL
light source : 300 W Xe lamp (300 < λ < 500 nm)

These finding confirm preferential introduction of O atoms from H_2O on the Pt/WO_3-K photocatalyst. Other Pt/WO_3 photocatalysts also preferentially generated phenol that contained O atoms originating from H_2O molecules (Figs. S7 and S8; Table 4, entries 2, 3, 10, 11), indicating that phenol production on Pt/WO_3 proceeded through •OH generation from H_2O (Scheme 1). As shown in Fig. S9, phenol production on Pt/WO_3-K was drastically suppressed by addition of a small amount of 2-propanol (188 μmol, 10 times greater than benzene), which is an efficient •OH scavenger. This adds additional evidence for the reaction scheme involving •OH radicals.

In contrast, the Pt/TiO_2 system produced appreciable amounts of phenol containing O atoms originating from O_2, along with others derived from H_2O, indicating that phenol production proceeded through a reaction pathway involving O_2 molecules (Scheme 2) in parallel with a pathway involving H_2O (Scheme 1). For example, photoirradiation of Pt/TiO_2-P in $H_2{}^{18}O$ with $^{16}O_2$ yielded a significant percentage of unlabeled phenol (*ca*. 33% at 15 min); the percentage was less than that of labeled phenol (Fig. 3; Table 4, entry 4). Interestingly, the percentage of unlabeled phenol increased with irradiation time (*ca*. 65% at 8 h), indicating that the contribution of the reaction pathway involving O_2 molecules became more dominant as the reaction progressed. Reaction in $H_2{}^{16}O$ with labeled $^{18}O_2$ also yielded a mixture of phenol molecules containing ^{16}O or ^{18}O (Fig. 4; Table 4, entry 12), in which the percentage of ^{18}O-labeled phenol molecules increased from 36 to 60% as the reaction proceeded. Phenol production on Pt/TiO_2-P was suppressed slightly by addition of 2-propanol, an •OH scavenger (Fig. S9). Thus, phenol production on Pt/TiO_2-P proceeded simultaneously *via* two different pathways (Schemes 1 and 2), while the contribution of the pathway involving O_2 gradually becomes dominant after prolonged irradiation time. Other Pt/TiO_2 photocatalysts, regardless of crystal phase (anatase or rutile), also produced a significant percentage of phenol molecules containing O atoms originating from O_2 (Figs. 3, 4, S6, S7; Table 4, entries 5, 6, 13, 14), while the change in percentage of ^{18}O-labeled phenol during the reaction differed significantly between Pt/TiO_2-A and Pt/TiO_2-R.

These results revealed that the Pt/WO_3 and Pt/TiO_2 systems possessed different reactivity toward oxidations as well as toward reductions. The holes generated on Pt/WO_3 photocatalysts reacted primarily with H_2O molecules, even in the presence of benzene in the aqueous solution, selectively generating •OH radicals that subsequently reacted with benzene to produce phenol. However, a portion of the holes generated on Pt/TiO_2 photocatalysts reacted directly with benzene molecules adsorbed on the TiO_2 surfaces, not only with H_2O, to generate cationic radical benzene species, which subsequently reacted with O_2 (or $\bullet O_2^-$) and protons to produce phenol.

3.4. Reaction mechanisms for phenol production on Pt/WO_3 and Pt/TiO_2

The holes generated in WO_3 and TiO_2 demonstrate distinctly different reactivity toward hydroxylation and oxidation of benzene in water. Since the oxidative potential of the holes generated in WO_3 and TiO_2 are essentially the same due to similarities in their valence band maximums,[45, 46] the different

levels of reactivity for oxidation was likely due to the different adsorption states of benzene molecules on the surface of the photocatalyst in water. The adsorption state of benzene molecules from the gas phase onto the surface of the photocatalyst was investigated using FT-IR, while it is an indirect method for investigating the adsorbed states of benzene in aqueous solutions. The spectra before adsorption of benzene on WO_3-K (10 m^2 g^{-1}) and TiO_2-A (10 m^2 g^{-1}) was subtracted from the corresponding spectra after adsorption. The spectrum of benzene in the gas phase also is shown for comparison. As shown in Fig. S10, only weak peaks corresponding to adsorbed benzene molecules were observed on WO_3-K sample at wavenumbers similar to those of benzene molecules in the gas phase, indicating that only a small number of benzene molecules adsorbed physically on the surface of WO_3-K particles. In contrast, intense IR band corresponding to benzene molecules adsorbed on TiO_2-A were observed at wavenumbers (1440–1540 cm^{-1}) slightly lower than those of benzene molecules in the gas phase. In addition, the IR band derived from surface hydroxyl groups of TiO_2-A, originally observed at approximately 3500–3800 cm^{-1}, decreased after benzene adsorption. This result indicated that the benzene molecules were strongly adsorbed to the TiO_2-A surface through interactions with surface hydroxyl groups, whereas benzene molecules were only physically adsorbed onto the WO_3 surface through weak interactions.

These results shown above led to the proposed reaction mechanism for direct hydroxylation of benzene to phenol in the Pt/WO_3 and Pt/TiO_2 systems as illustrated in Fig. 5. Since only small amount of benzene molecules were physically adsorbed on the WO_3 surface, the photo-generated holes in the WO_3 photocatalyst react primarily with H_2O molecules, even in the presence of benzene molecules in the aqueous solution, yielding •OH radicals that subsequently react with benzene to produce phenol with high selectivity. At the same time, the photoexcited electrons on Pt/WO_3 photocatalysts react with molecular O_2 to generate mainly H_2O_2 on the Pt cocatalyst. The H_2O_2 generated is readily decomposed into H_2O and O_2 on the Pt cocatalyst and therefore has little impact on the hydroxylation and oxidation of benzene. In contrast, a considerable number of holes generated on Pt/TiO_2 photocatalysts react directly with benzene molecules that are strongly adsorbed on the surface *via* interactions with surface hydroxyl groups, generating cationic radical benzene species. These radicals subsequently react with O_2 (or $•O_2^-$) to give peroxyl radicals that then reductively react with photoexcited electrons and protons to produce phenol. Since these peroxyl radicals are generally unstable and spontaneously decompose, the formation of peroxyl radicals might be a reason for the low selectivity of TiO_2 for phenol. The adsorption of benzene molecules on the surface of TiO_2 undoubtedly increases the possibility of direct oxidation of benzene into cleaved intermediates leading to CO_2 as the final product due to the holes. This direct decomposition pathway is supported by the noticeable production of CO_2 in the initial period of photoirradiation on Pt/TiO_2-P as seen in Fig. 1. Additionally, the photoexcited electrons on TiO_2 reduce O_2 into radical species such as $•O_2^-$ or $•HO_2$, which subsequently contribute to the oxidative decomposition of benzene and its intermediates. Both the direct oxidation of substrates (*e.g.*, phenol) on the TiO_2 surface and oxidation by oxygen radical species are the main reasons for reduced phenol selectivity on TiO_2. In contrast, these two oxidation pathways are inhibited by WO_3 system, enabling the Pt/WO_3 photocatalysts to produce phenol with high selectivity in the presence of H_2O and O_2.

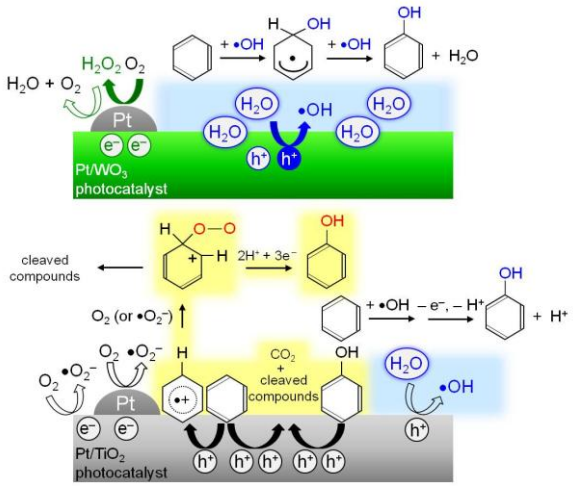

Figure 5. Proposed reaction mechanisms for phenol production over Pt/WO_3 and Pt/TiO_2 photocatalysts.

The main property of Pt/WO_3 photocatalysts that enables highly selective phenol production is the selective generation of •OH radicals, even in the presence of organic substances such as benzene in water. When reaction on Pt/WO_3 was initiated with 10-fold greater concentration of benzene (25 mmol L^{-1}), the amount of phenol produced only increased by *ca*. 16% (see Fig. S11). Note that the results of ^{18}O-labeled reactions with a much higher concentration of benzene (500 mmol L^{-1}) indicated the preferential oxidation of water molecules on Pt/WO_3 photocatalysts. These results confirmed that the surface of WO_3 has properties that promote preferential oxidation of water molecules, even in the presence of significantly high concentration of benzene molecules, generating •OH radicals that are effective for selective phenol synthesis.

The specific surface area and the difference in the density of hydroxyl groups on the sample surface were considered as reasons for the differences in properties between WO_3 and TiO_2 for adsorption of benzene and its intermediates. However, the Pt/WO_3-K and the Pt/TiO_2-A samples, which have similar surface areas (*ca*. 10 m^2 g^{-1}), had different reactivities. A series of WO_3 samples with different densities of hydroxyl groups as well as the surface areas, was prepared by calcination of tungstic acid at various temperatures (XRD patterns: Fig. S12; IR spectra: Fig. S13), and employed as photocatalysts in the reactions with isotopically labeled $^{18}O_2$. As shown in Table S1, the percentage of labeled phenol produced for each sample was similar, indicating that the density of surface hydroxyl groups was not the main cause of reactivity differences between WO_3 and TiO_2 systems for the oxidative process. Although the dominant property enabling the WO_3 system to produce phenol with high selectivity remains unclear and needs clarification, the unique properties of WO_3 photocatalysts for achieving highly selective phenol production in the presence of molecular O_2 probably promote practically useful organic syntheses using photocatalysis.

4. Conclusions

Highly selective phenol synthesis directly from benzene was demonstrated using Pt-loaded WO_3 photocatalysts in water containing molecular oxygen. Results revealed that the surface of WO_3, which is different from that of conventional TiO_2, enables preferential oxidation of water molecules even in the presence of considerably high concentration of benzene molecules in water, to selectively generate •OH radicals that promote selective phenol production. This finding indicates that the •OH radicals can be continuously generated by simple photoirradiation (utilizing visible light) of Pt/WO_3 photocatalysts in water in the presence of O_2; the •OH radicals generated can then be used for organic synthetic reactions in water if the reactant possesses low affinity toward the surface of WO_3. Both the efficiency and selectivity in the present system will be improved when the nature and the reaction mechanism on WO_3 photocatalyst is better understood. The present study demonstrates the possibility of environmentally benign photocatalytic processes with potential for reducing energy consumption of fine chemical production by harnessing the energy of artificial or natural sunlight.

Acknowledgement

This work was financially supported by JSPS-NEXT program. The authors are also indebted to technical division of Catalysis Research Center for their help in building experimental equipment.

Notes and references

[a] *Graduate School of Engineering, Kyoto University, Katsura, Nishikyo-ku, Kyoto 615-8510, Japan. Fax: +81-75383-2479; Tel: +81-75383-2479; E-mail: ryu-abe@scl.kyoto-u.ac.jp*
[b] *Catalysis Research Center, Hokkaido University, Sapporo 001-0021, Japan. Fax: +81-11706-9133; Tel: +81-11706-9132; E-mail: ohtani@cat.hokudai.ac.jp*
[c] *JSPS-NEXT Program, Koujimachi, Chiyoda-ku, Tokyo 102-0083, Japan.*

† Electronic Supplementary Information (ESI) available: Results on hydroxylation and oxidation of benzene on various photocatalyst under different conditions such as, photocatalysts loaded with different amount of Pt cocatalyst, irradiated in the aqueous solution with different pH values or different benzene concentrations, irradiated in the copresence of benzene and 2-propanol, are shown. IR spectra of photocatalyst samples after benzene adsorption, XRD pattern and raw IR spectra of WO_3 samples prepared from tungstic acid (WO_3-TA), and the results on the hydroxylation of benzene using oxygen stable isotope on WO_3-TA are also shown. See DOI: 10.1039/b000000x/

1 M. Fujihira, Y. Satoh and T. Osa, *Nature*, 1981, **293**, 206.
2 M.-R. Hoffmann, S.-T. Martin, W.-Y. Choi and D.-W. Bahnemann, *Chem., Rev.*, 1995, **95**, 69.
3 V. Augugliaro and L. Palmisano, *ChemSusChem*, 2010, **3**, 1135.
4 C.-D. Jaeeger and A.-J. Bard, *J. Phys. Chem.*, 1979, **83**, 3146
5 H. Noda, K. Oikawa, H. Kamada, *Bull. Chem. Soc. Jpn.*, 1992, **65**, 2505.
6 L. Sun and J.-R. Bolton, *J. Pys. Chem.*, 1996, **100**, 4127
7 K. Ishibashi, A. Fujishima, T. Watanabe and K. Hashimoto, *Electrochem. Commun.*, 2000, **2**, 207
8 H. Czili and A. Horvath, *Appl. Catal. B: Environ.*, 2008, **81**, 295
9 D.-F. Ollis, C.-J. Hsiao, L. Budiman and C.-L. Lee, *J. Catal.*, 1984, **88**, 89.
10 Y. Sun and J.-J Pignatello, *Environ. Sci. Technol.*, 1995, **29**, 2065.
11 H. Einaga, S. Futamura, T. Ibusuki, *Appl. Catal. B: Environ.*, 2002, **38**, 215.
12 A. Fujishima, T.-N. Rao and D.-A. Tryk, *J. Photochem. Photobiol. C: Photochem. Rev.*, 2000, **1**, 1.
13 R. Asahi, T. Morikawa, K. Aoki and Y. Taga, *Science*, 2001, **293**, 269.
14 T. Ohno, K. Sarukawa and M. Matsumura, *New J. Chem.*, 2002, **26**, 1167.
15 R. Inaba, T. Fukahori and M. Hamamoto, *J. Mol. Catal. A: Chem.*, 2006, **260**, 247.
16 T. Morikawa, Y. Irokawa and T. Ohwaki, *Appl. Catal. A: Gen.*, 2008, **314**, 123.
17 H. Irie, K. Kamiya, T. Shibanuma, S. Miura, Donald A. Tryk, T. Yokoyama and K. Hashimoto, *J. Phys. Chem. C*, 2009, **113**, 10761.
18 O.-O. P. Mahaney, N. Murakami, R. Abe and B. Ohtani, *Chem. Lett.*, 2008, **37**, 216.
19 G. Palmisano, V. Augugliaro, M. Pagliaro and L. Palmisano, *Chem. Commun.* 2007, 3425.
20 M. Zhang, Q. Wang, C. Chen, L. Zang, W. Ma and J. Zhao, *Angew. Chem. Int. Ed.*, 2009, **48**, 6081.
21 G. Zhang, J. Yi, J. Shim, J. Lee and W. Choi, *Appl. Catal. B: Environ.*, 2011, **102**, 132
22 T. D. Bui, A. Kimura, S. Ikeda, and M. Matsumura, *Appl. Catal. B: Environ.*, 2010, **94**, 186.
23 R. Dietz, A.-E. J. Forno, B.-E. Larcombe and M.-E. Peover, *J. Chem. Soc. B,* 1970, 816.
24 M.-J. Gibian, D-T. Sawyer, T. Ungermann, R. Tangpoonpholvivat and M.-M. Morrison, *J. Am. Chem. Soc.*, 1979, **101**, 640.
25 D.-T. Sawyer, *Acc. Chem. Res.*, 1981, **14**, 393.
26 M.-A. Fox, *Acc. Chem. Res.*, 1983, **16**, 314.
27 J. Schwitzgebel, J.-G. Ekerdt, H. Gerischer and A. Heller, *J. Phys. Chem.*, 1995, **99**, 5633.
28 Y. Ohko, D.-A. Tryk, K. Hashimoto and A. Fujishima, *J. Phys. Chem. B*, 1998, **102**, 2699.
29 H. Lee and W. Choi, *Environ. Sci. Technol.*, 2002, **36**, 3872
30 Y. Li., J. Niu., L. Yin, W. Wang, Y. Bao, J. Chen and Y. Duan, *J. Environ. Sci.*, 2011, **23**, 1911
31 Y. Shiraishi, Y. Sugano, and T. Hirai, *Angew. Chem. Int. Ed.*, 2010, **49**, 1656.
32 H. Yoshida, H. Yuzawa, M. Aoki, and T. Hattori, *Chem. Commun.*, 2008, 4634
33 H. Yuzawa, M. Aoki, K. Otake, T. Hattori, H. Itoh, and H. Yoshida, *J. Phys. Chem. C*, 2012, **116**, 25376
34 Pal, S. Ikeda, H. Kominami, B. Ohtani, *J. Catal.*, 2003, **217**, 152
35 R. Abe, H. Takami, N. Murakami and B. Ohtani, *J. Am. Chem. Soc.*, 2008, **130**, 7780.
36 O. Tomita, R. Abe and B. Ohtani, *Chem. Lett.*, 2011, **40**, 1405.
37 C. Kormann, D.-W. Bahanemann, M.-R. Hoffmann, *Environ. Sci. Technol.* 1988, **22**, 798.
38 D.-S. Arnold', C.-A. Plank, E.-E. Erickson and F.-P. Pike, *Ind. Eng. Chem. Chem. Eng. Data* Series, 1958, **3,** 253.
39 L.-A. Lyon and J.-T. Hupp, *J. Phys. Chem. B.*, 1999, **103**, 4623.
40 C. Walling, *Acc Chem. Res.*, 1975, **8**, 125.
41 W. Matthews, *J. Chem. Soc. Faraday Trans. 1*, 1984, **80**, 457.
42 S. Goldstein, G. Czapski and J. Rabani, *J. Phys. Chem.*, 1994, **98**, 6586.
43 T.-D. Bui, A. Kimura, S. Ikeda and M. Matsumura, *J. Am. Chem. Soc.*, 2010, **132**, 8453.
44 Y. Li, B. Wen, C. Yu, C. Chen, H. Ji, W. Ma and J. Zhao, *Chem. Eur. J.*, 2012, **18**, 2030.
45 D.-E. Scaife, *Solar Energy*, 1980, **25**, 41.
46 M. Miyauchi, A. Nakajima, T. Watanabe and K. Hashimoto, *Chem. Mater.*, 2002, **14**, 4714.

Supporting Information

Highly selective phenol production from benzene on platinum-loaded tungsten oxide photocatalyst with water and molecular oxygen: Selective oxidation of water by holes for generating hydroxyl radical as predominant source of hydroxyl group

Osamu Tomita,[a,b] Bunsho Ohtani[b] and Ryu Abe*[a,c]

[*]*Graduate School of Engineering, Kyoto University, Katsura, Nishikyo-ku, Kyoto 615-8510, Japan*

[†]*Catalysis Research Center, Hokkaido University, Sapporo 001-0021, Japan*

[‡]*JSPS-NEXT Program, Koujimachi, Chiyoda-ku, Tokyo 102-0083, Japan*

E-mail: ryu-abe@scl.kyoto-u.ac.jp

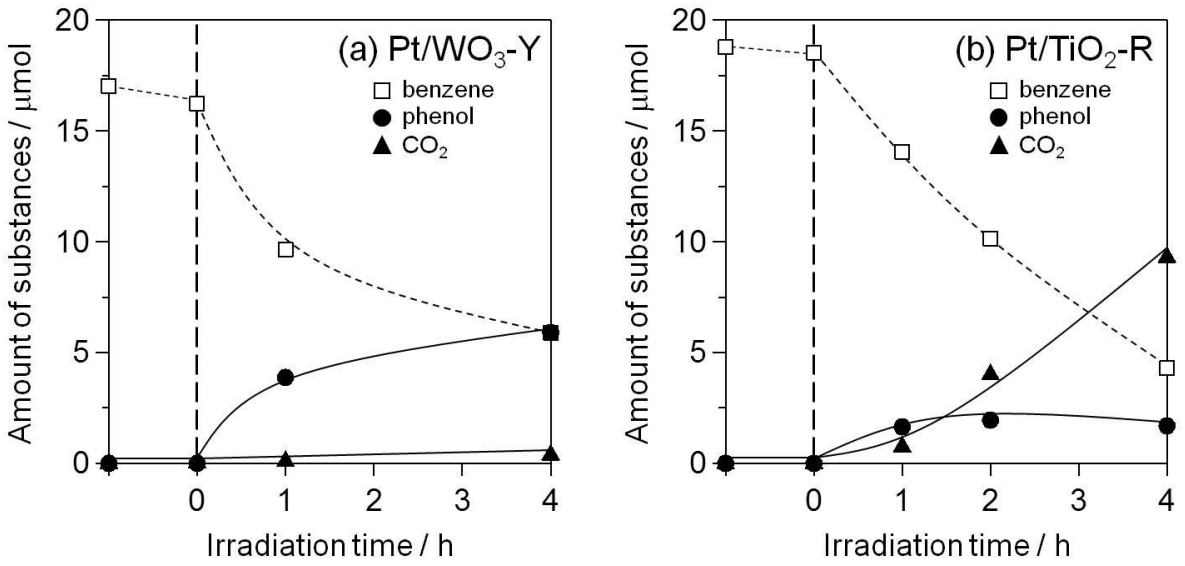

Figure S1. Time course of hydroxylation and oxidation of benzene over (a) Pt/WO_3-Y and (b) Pt/TiO_2-R photocatalysts in aerated aqueous solutions of benzene (18.8 μmol) under ultraviolet and visible light irradiation ($300 < \lambda < 500$ nm).

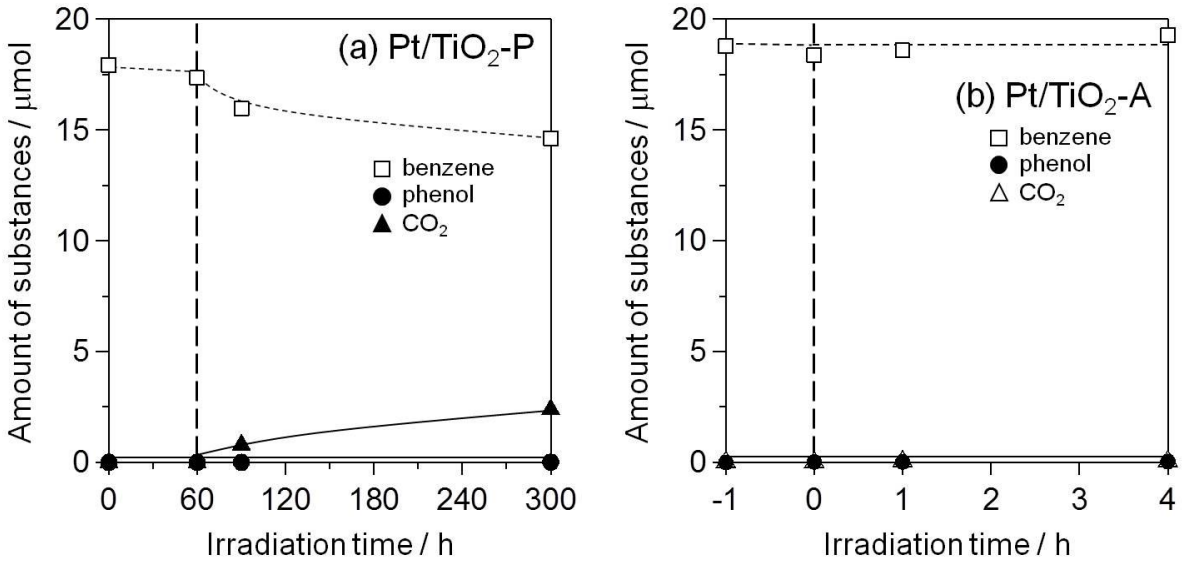

Figure S2. Time course of photocatalytic oxidation of benzene over (a) Pt/TiO_2-P and (b) Pt/TiO_2-A photocatalysts in aerated aqueous solutions of benzene (18.8 μmol) under visible light irradiation ($400 < \lambda < 500$ nm).

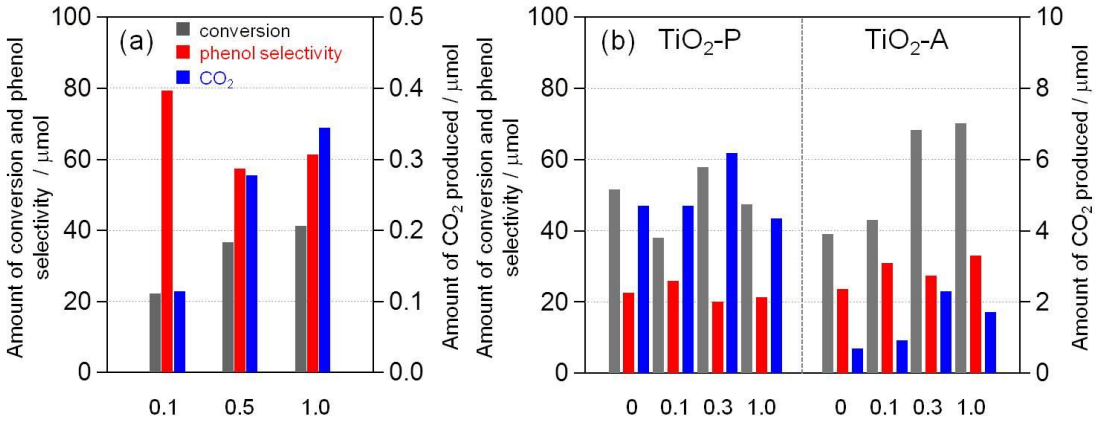

Figure S3. Influence of Pt amount on the amount of conversion, phenol selectivity, and amount of CO_2 on (a) Pt/WO_3-K and (b) TiO_2 photocatalyst during hydroxylation of benzene (irradiation time 1 h).

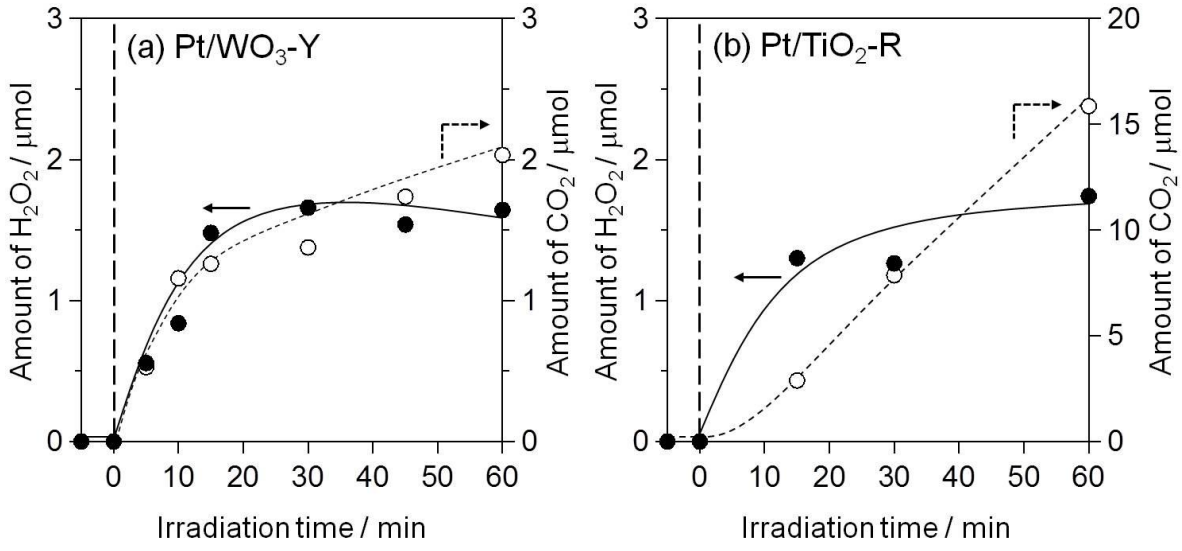

Figure S4. Time course curves of H_2O_2 and CO_2 generation over (a) Pt/WO_3-Y and (b) Pt/TiO_2-R photocatalysts suspended in AcOH solution under ultraviolet and visible light irradiation ($300 < \lambda < 500$ nm).

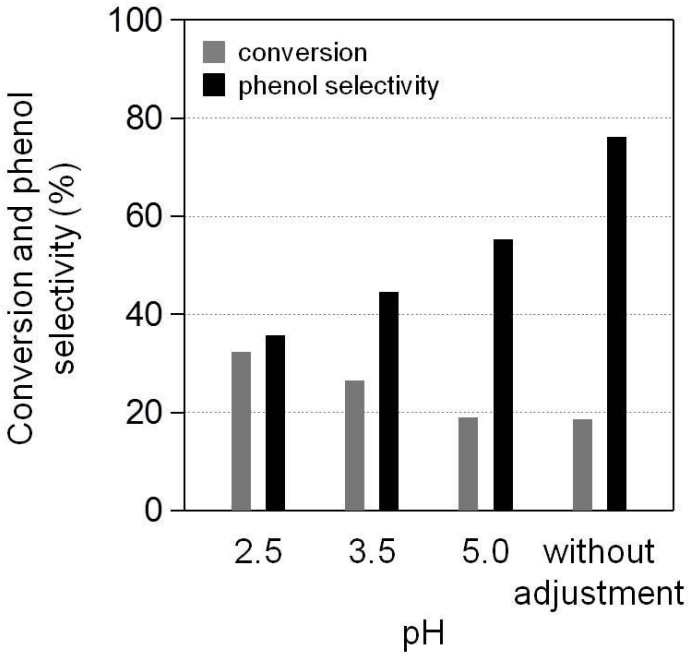

Figure S5. Dependence of photocatalytic hydroxylation of benzene on pH for use of Pt/WO_3-K photocatalyst.

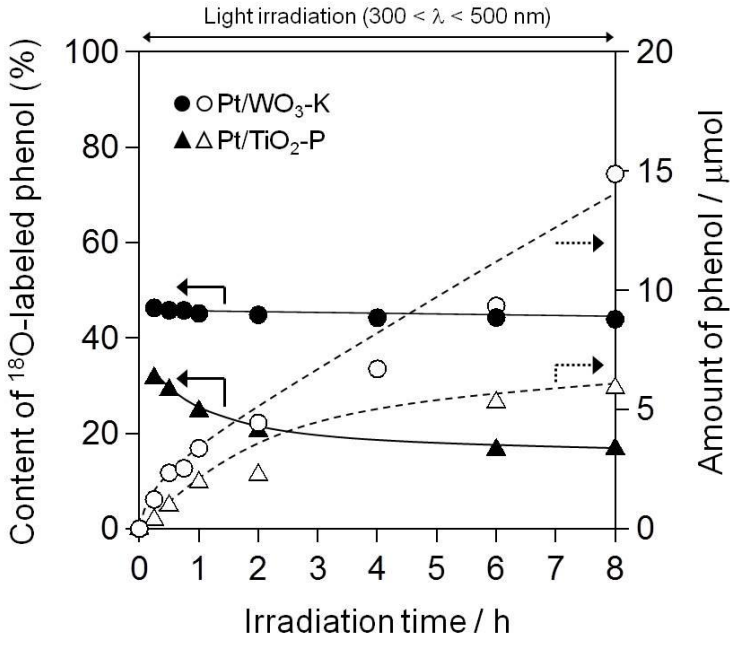

Figure S6. Time course of photocatalyzed phenol productionfrom benzene on Pt/WO_3-K and Pt/TiO_2-P samples. Reactions were conducted in $H_2{}^{16}O$-$H_2{}^{18}O$ mixed solvent containing benzene and normal molecular $^{16}O_2$.

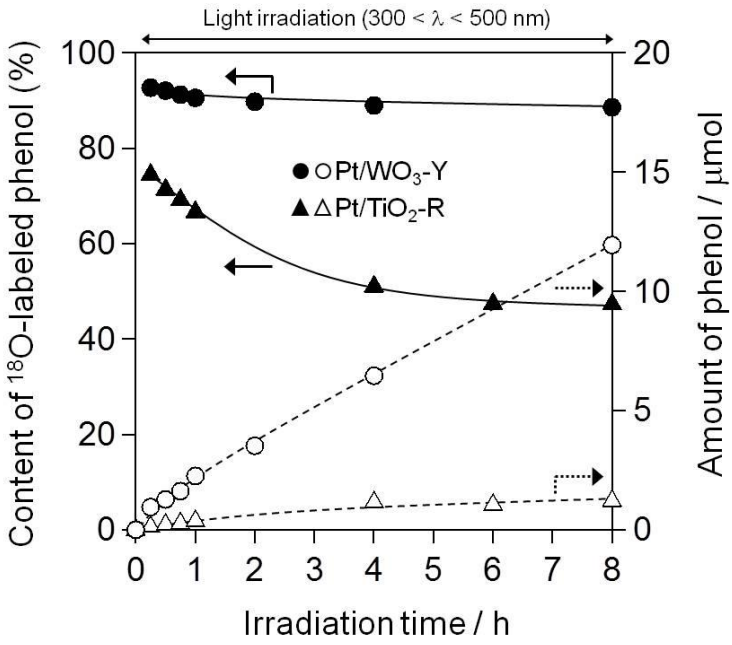

Figure S7. Time course of photocatalyzed phenol production from benzsene on Pt/WO_3-Y and Pt/TiO_2-R samples. Reactions were conducted in ^{18}O-enriched water (98% $H_2{}^{18}O$) containing benzene and normal molecular $^{16}O_2$.

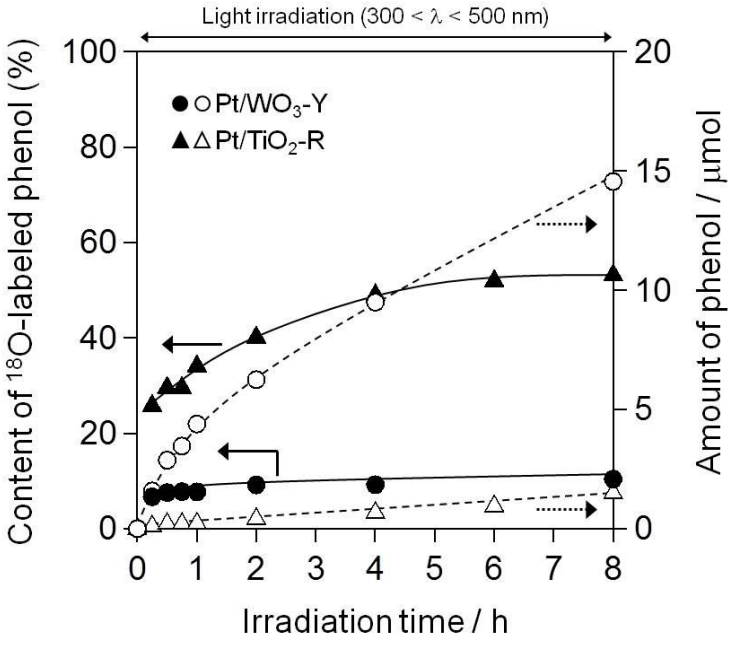

Figure S8. Time course of photocatalyzed phenol production from benzene on Pt/WO_3-Y and Pt/TiO_2-R samples. Reactions were conducted in normal water ($H_2{}^{16}O$) containing benzene and molecular $^{18}O_2$.

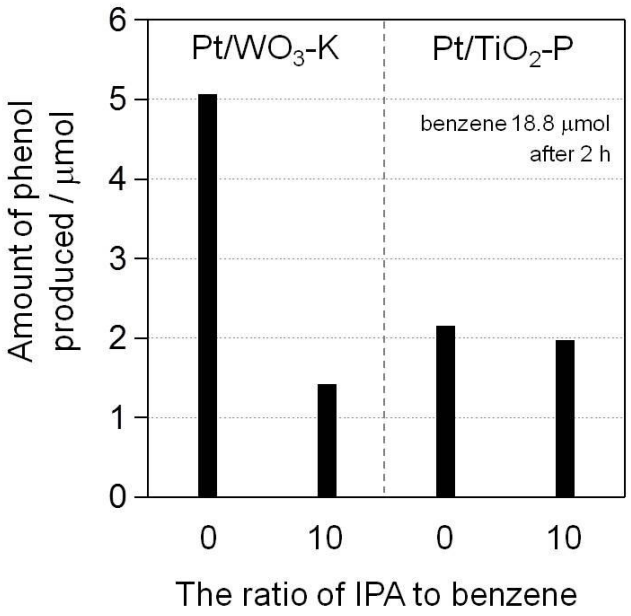

Figure S9. Amount of phenol produced from hydroxylation of benzene in the presence of IPA over Pt/WO_3-K and Pt/TiO_2-P photocatalysts.

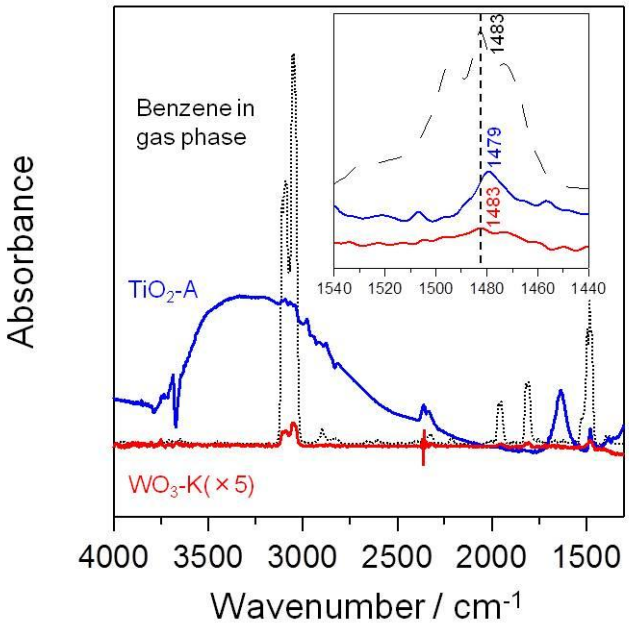

Figure S10. FT-IR subtraction spectra of benzene on photocatalysts.

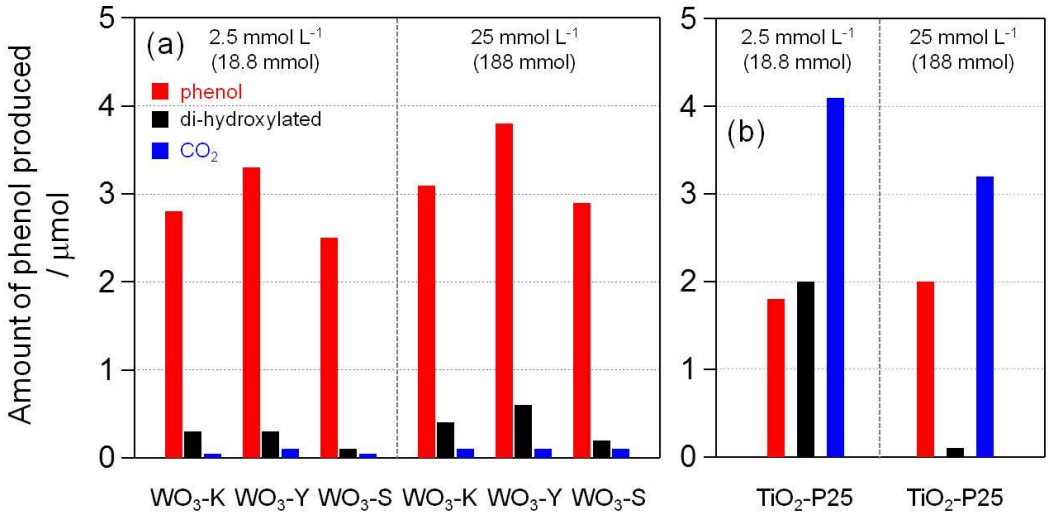

Figure S11. Influence of initial concentration of benzene on the amount of phenol, di-hydroxylated benzene and CO_2 on (a) Pt/WO_3 and (b) TiO_2 photocatalysts during hydroxylation of benzene (Pt: 0.1 wt.%).

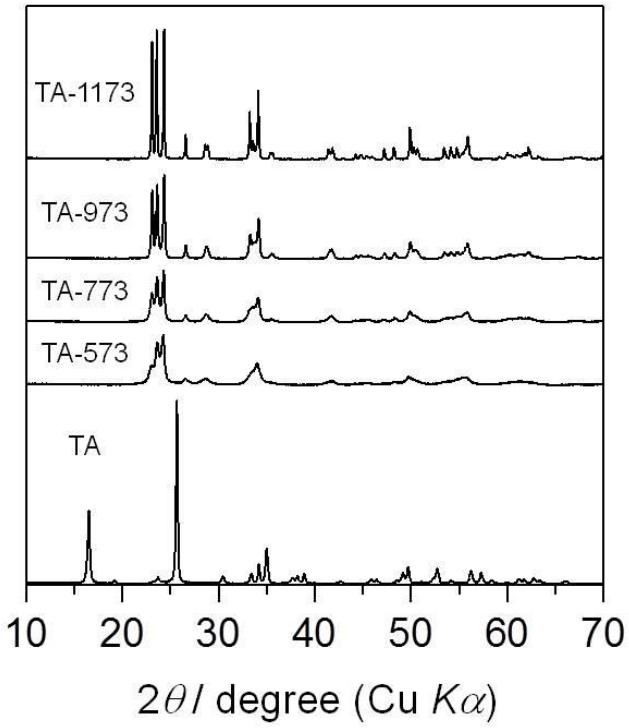

Figure S12. XRD pattern of WO_3 samples obtained from tungstic acid (H_2WO_4, TA) as the W precursor.

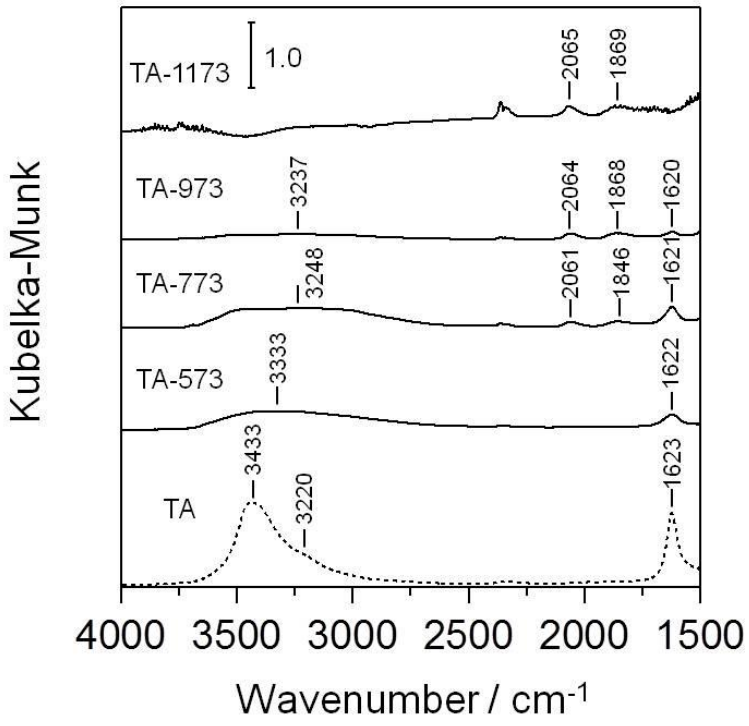

Figure S13. IR spectra of WO_3 samples obtained from tungstic acid (H_2WO_4, TA) as the W precursor.

Table S1. Direct hydroxylation of benzene to phenol on WO_3-TA (prepared by calcination of tungstic acid powder) in normal water ($H_2{}^{16}O$) containing benzene and molecular $^{18}O_2$.

Entry	Calcination temperature / K	Content of labeled phenol (%) (Amount of phenol produced / μmol)	
		1 h	8 h
1	573	95.1 (0.6)	95.2 (2.5)
2	773	94.4 (1.2)	92.0 (3.8)
3	973	96.3 (1.3)	93.3 (4.9)
4	1173	94.9 (0.9)	94.0 (2.2)

Initial concentration of benzene : 500 μmol, Amount of solvent : 1.0 mL

Light source : 300 W Xe lamp (300 < l < 500 nm)